Evaluation of off-axis wedge correction factor using diode dosimeters for estimation of delivered dose in external radiotherapy

Mahmoud Allahverdi, Alireza Mohammadkarim[1], Mahbod Esfehani[2], Hasanali Nedaie[3], Alireza Shirazi, Ghazale Geraily

Department of Medical Physics, Tehran University of Medical Sciences, [1]Department of Medical Radiation Engineering, Science and Research Branch, Islamic Azad University, [2]Radiotherapeutic Oncology Department of Cancer Institute, [3]Department of Radiotherapy, Tehran University of Medical Sciences, Tehran, Iran

ABSTRACT

An *in vivo* dosimetry system, using p-type diode dosimeters, was characterized for clinical applications of treatment machines ranging in megavoltage energies. This paper investigates two different models of diodes for externally wedged beams and explains a new algorithm for the calculation of the target dose at various tissue depths in external radiotherapy. The values of off-axis wedge correction factors were determined at two different positions in the wedged (toward the thick and thin edges) and in the non-wedged directions on entrance and exit surfaces of a polystyrene phantom in ^{60}Co and 6 MV photon beams. Depth transmission was defined on the entrance and exit surfaces to obtain the off-axis wedge correction factor at any depth. As the sensitivity of the diodes depends on physical characteristics [field size, source–skin distance (SSD), thickness, backscatter], correction factors were applied to the diode reading when measuring conditions different from calibration situations. The results indicate that needful correction factors for ^{60}Co wedged photons are usually larger than those for 6 MV wedged photon beams. *In vivo* dosimetry performed with the proposed algorithms at externally wedged beams has negligible probable errors (less than 0.5%) and is a reliable method for patient dose control.

Key words: Diode dosimeter, external radiotherapy, *in vivo* dosimetry, ionization chamber, off-axis wedge correction factor

Introduction

In vivo dosimetry is widely considered to be an important tool for quality assurance in external radiotherapy.[1-4] International Commission of Radiological Units and Measurements (ICRU) reports pointed to a need for accuracy of ±5% in the delivery of the absorbed dose to a target volume in a patient.[5,6] The *in vivo* diode probe is a detector to be used clinically for dose verification during external megavoltage photon beam therapy. A routine diode in *in vivo* dosimetry is based on a combination of entrance and exit dose measurements.[1,7-9] *In vivo* dosimetry has shown to be useful for detecting errors that would have passed through the treatment chain unnoticed and affected patient outcome.[6,10]

Before any routine use of *in vivo* diode probes, a set of initial studies is required. These consist of the measurement of calibration and correction factors (CFs), checking the system, methodology and the use of the factors in practice; and clinical pilot studies to establish the existing accuracy and precision of given treatment situation.[11-13] The ideal diode for *in vivo* dosimetry should show minimal dependence on field size, source–skin distance (SSD) and interposition of modifying devices such as wedges.[1,4,14] CFs need to be modified with accumulating dose.

Wedge filters ideally modify photon intensities in only one direction. However, in the non-wedged direction, the intensity is affected too; it usually decreases with increasing off-axis distance.[15]

Address for correspondence:
Dr. Mahmoud Allahverdi,
Department of Medical Physics, Tehran university of Medical Sciences, Tehran, Iran.
E-mail: alahverdi@sina.tums.ac.ir

According to previous studies, wedge CFs of ionization chamber dosimeters in different wedge directions at various off-axis distances were different from those at central axis,[15] while in other studies carried out by diode dosimeters, no differences between them were considered.[1,6,7] So, it is necessary to investigate the response of diodes at different directions of externally wedged fields. The importance of this statement becomes clearer when considering that in the past, *in vivo* dosimetry papers, where the entrance and exit surface diodes were used in order to determine target dose, one of the diodes was shifted out of central beam axis to avoid shadow effect.[6,9] Moreover, sometimes it is necessary to determine the delivered dose to organ at risk placed off axis, from surface doses in wedged fields. In this case, most previous studies supposed that the target was exactly at the middle of entrance and exit surfaces and several approximate methods were implemented,[1,6,16-18] although target or organ at risk is not exactly at the middle of entrance and exit surfaces. It seems that a new algorithm is necessary for improving the dose estimation accuracy in wedged fields.

In this paper, the off-axis wedge CF (OAWCF) was evaluated by different arrangements of wedge directions on entrance and exit surfaces of a polystyrene phantom. This research presents a systematic study of the influences of OAWCFs, in different field sizes and SSDs, for ^{60}Co and 6 MV photons, for dose values, and then suggests a method to estimate the dose value in any depth of the tissue.

Materials and Methods

The investigations were performed using ^{60}Co photon beams generated by a Teratron 780C ^{60}Co treatment machine and 6 MV photon beams generated by a Varian Clinac 2100C. T60010L model (p-type diodes for 1–5 MV photon energies with a 1-cm water equivalent build-up cap) and T60010M model (p-type diodes for 5–13 MV photon energies with a 2-cm water equivalent build-up cap) of PTW diodes were used for ^{60}Co and 6 MV photon beams, respectively. OAWCF values were determined under different physical conditions for use in clinical *in vivo* dosimetry.

For calibration of diodes, they were first placed on the entrance and exit surfaces of a 15-cm polystyrene phantom under reference conditions (i.e. field size = 10 × 10 cm^2; SSD = 80 cm for ^{60}Co photon beams; SSD = 100 cm for 6 MV photon beams). Calibrations were performed individually for each diode against an ionization chamber detector (TM31013 and TM30010 models of PTW ionization chambers were used as the reference detectors for ^{60}Co and 6 MV photon beams, respectively). To calculate a target dose at a defined tissue depth, at first, a variety of calibration factors must be considered for each diode. The entrance dose calibration factor ($F_{cal,en}$) was determined as the ratio of the absorbed

dose measured by the ionization chamber (D) at the build-up depth ($d_{m,en}$) to the entrance semiconductor signal reading (R) on the surface with a build-up layer under reference conditions:[2,4,6,8,9] Similarly, the exit dose calibration factor ($F_{cal,ex}$) was determined as the ratio of the absorbed dose measured by the ionization chamber at the build-down (from the lack of backscatter radiation) depth ($d_{m,ex}$) to the exit diode signal reading on the surface with a build-up layer under reference conditions:[2,6,8,9] The CFs for non-standard irradiation conditions were determined like in previous studies.[6,19]

The OAWCF under reference conditions can be defined as:

$$OAWCF = [(D/R)_{wedged\ beam} / (D/R)_{open\ beam}] = \left[\left(\frac{D_{wedged\ beam}}{D_{open\ bean}} \right) \Big/ \left(\frac{R_{wedged\ beam}}{R_{open\ beam}} \right) \right] \ ...(1)$$

For non-reference conditions of defined field size (*f.s*), the OAWCFs on the entrance and exit surfaces are given by:

$$OAWCF_{en} = \left[\frac{D(w, f.s)}{D(open, f.s_{ref})} \right]_{en} \div \left[\frac{R(w, f.s)}{R(open, f.s_{ref})} \right]_{en} \ ......(2)$$

$$OAWCF_{ex} = \left[\frac{D(w, f.s)}{D(open, f.s_{ref})} \right]_{ex} \div \left[\frac{R(w, f.s)}{R(open, f.s_{ref})} \right]_{ex} \ ...(3)$$

The relevant transmission factors for each depth were entrance depth transmission ($T_{d,en}$) and exit depth transmission ($T_{d,ex}$). $T_{d,en}$ was estimated as the ratio of absorbed dose measured at any depth (D_d) to the absorbed dose that was measured at build-up depth ($D_{m,en}$). Therefore,

$$T_{d,en} = \frac{D_d}{D_{m,en}} = (Percentage\ Depth\ Dose)_d = PDD_d \ .(4)$$

$T_{d,ex}$ was estimated as the ratio of absorbed dose in any depth (D_d) to the absorbed dose at the build-down depth ($D_{m,ex}$). Therefore,

$$T_{d,ex} = \frac{D_d}{D_{m,ex}} = \frac{D_d / D_{m,en}}{D_{m,ex} / D_{m,en}} = \frac{(Percentage\ Depth\ Dose)_d}{(Percentage\ Depth\ Dose)_{ex}} = \frac{PDD_d}{PDD_{ex}} \ ....(5)$$

To obtain the OAWCF at any depth ($OAWCF_{d,en}$) from the $OAWCF_{en}$, $OAWCF_{en}$ can be multiplied by $T_{d,en}$:

$$OAWCF_{d,en} = OAWCF_{en} \times PDD_d \ .... (6)$$

Also, to evaluate the OAWCF at any depth ($OAWCF_{d,ex}$) from the $OAWCF_{ex}$, $OAWCF_{ex}$ can be multiplied by $T_{d,ex}$:

$$OAWCF_{d,ex} = OAWCF_{ex} \times \frac{PDD_d}{PDD_{ex}} \ ....(7)$$

According to other investigations, percentage depth dose (PDD) values of wedged fields in all directions at different off-axis distances are approximately equal to those of open fields at central axis.[15,20] So, PDD values of open fields at

central axis were used in the above equations.

Under complete photon backscatter conditions, the exit dose is not measured. Therefore, a backscatter factor (BSF) was determined as the ratio of the ionization chamber reading under full backscatter conditions (R_{FB}) to the ionization chamber reading under exit-dose measurement conditions (R_{MC}) for different values of field size.[9]

Target dose at any depth of the patient of wedged fields in clinical applications can be deduced from the diode reading at the entrance and exit surfaces of the patient ($R_{r,en}$ and $R_{r,ex}$) multiplied by proper calibration factor and OAWCF ($OAWCF_{d,en}$ and $OAWCF_{d,ex}$):

$$D_{target} = F_{cal,en} \times R_{r,en} \times OAWCF_{d,en} \quad ....(8)$$

$$D_{target} = F_{cal,ex} \times R_{r,ex} \times OAWCF_{d,ex} \quad ....(9)$$

To reduce statistical error, the target dose (D_{target}) can be concluded from averaging of equations (8) and (9).

In our proposed algorithm which is illustrated in [Figure 1], after dose measurements using entrance and exit diodes, $OAWCF_{en}$ and $OAWCF_{ex}$ are applied respectively on entrance and exit dose values for the corresponding field size by considering the direction and quantity of diode positioning out of central beam axis. Then, if SSD is different from reference SSD, SSD CFs are applied on the obtained entrance and exit doses.

In the next step, the entrance and exit transmission factors (equations 4 and 5) are applied on entrance and exit dose values. By means of this, PDD tables must be used to address ^{60}Co and 6 MV photon beams of any field size. It should be noticed that the PDD values are strongly affected by SSD. Therefore, to determine PDD_d (and PDD_{ex}) at
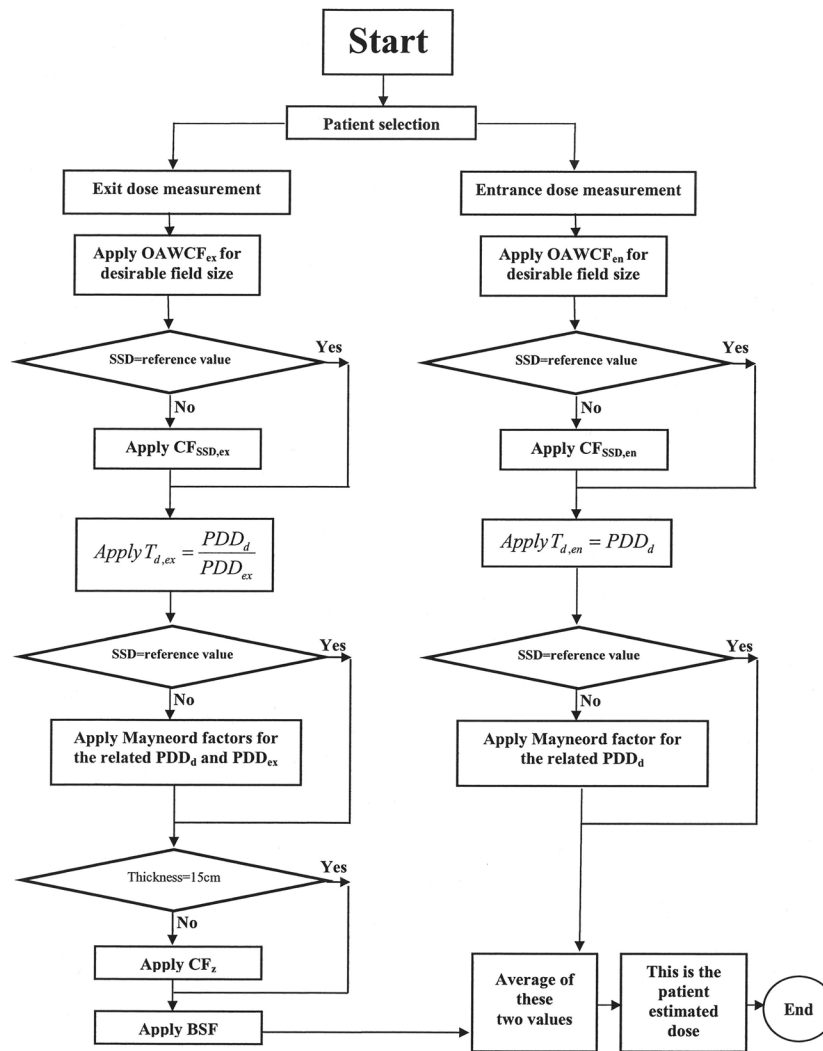

Figure 1: Method of estimating target dose at desirable depth in clinical measurements

non-reference SSDs, the Mayneord factor is needed.[21] In other words, PDD$_d$ (at non-reference SSD) = (Mayneord factor) × PDD$_d$ (at reference SSD).

These factors for ^{60}Co photons and 6 MV photons are equal to the following:

For ^{60}Co photons: Mayneord factor $= \left(\frac{SSD+0.5}{80.5}\right)^2 \left(\frac{80+d}{SSD+d}\right)^2$

For 6 MV photons: Mayneord factor $= \left(\frac{SSD+1.6}{101.6}\right)^2 \left(\frac{100+d}{SSD+d}\right)^2$

In the next step, if the patient thickness is different from reference thickness (15 cm), the thickness CF is applied on exit dose value; otherwise, it goes to the next step. After that, the BSF is applied on it. Finally, the arithmetic mean of entrance and exit dose values is calculated.

In this study, the entire diode and ionization chamber measurements were performed three times and the average of them was calculated to reduce statistics errors.

To check the accuracy of this algorithm, depth doses at different off-axis points within phantom were measured directly with ionization chamber. Calculated doses were acquired from entrance and exit diode readings corresponding to each point and applying them into the algorithm.

Results

Off-axis CF (CF$_{off-axis}$)

The off-axis CFs with the open field were measured for ^{60}Co and 6 MV photon beams on the entrance and exit points [Table 1]. The results illustrate that deviation of entrance off-axis CFs (CF$_{off,en}$) for ^{60}Co and 6 MV photon beams is less than ± 1% for reference open field sizes. On the other hand, the results illustrate that deviation of exit off-axis CFs (CF$_{off,ex}$) for ^{60}Co and 6 MV photon beams (for reference open field sizes) is within ±2%.

Off-axis wedge CF

The OAWCF was determined for ^{60}Co and 6 MV photon beams on the entrance and exit surfaces of a polystyrene phantom. We obtained the estimated values of OAWCF$_{en}$ and OAWCF$_{ex}$ for 30°, 45° and 60° physical wedges using

^{60}Co photons, with the maximum possible square field size available for these wedges (10 × 10 cm^2) on the entrance and exit surfaces of the phantom [Figure 2]. The results were obtained both in the wedged direction (positive direction: toward the thick edge, negative direction: toward the thin edge) and in the non-wedged direction. The OAWCF$_{en}$ and OAWCF$_{ex}$ were determined for 15°, 30°, 45° and 60° physical wedges also using 6 MV photon beams with the maximum possible square field usable for all of them (15 × 15 cm^2). The results for 6 MV photons are shown in [Figure 3].

Figure 2a shows that maximum variations of the OAWCF$_{en}$ for ^{60}Co photons at a 10 × 10 cm^2 field size in the wedged and non-wedged directions are 16 and 6%, respectively. Figure 3a shows that the maximum variation of OAWCF$_{en}$ for 6 MV photons at a 15 × 15 cm^2 field size in the non-wedged direction is about 1%. Also, the maximum variation of OAWCF$_{en}$ at this field size in the wedged direction is 4.7%.

It can be seen from Figures 2b and 3b that the maximum variations of OAWCF$_{ex}$ in the wedged direction for ^{60}Co and 6 MV photons are 8 and 6.8%, respectively, and the maximum variations of OAWCF$_{ex}$ in the non-wedged direction for ^{60}Co and 6 MV photons are 4 and 2%, respectively.

Moreover, the values of OAWCF$_{en}$ and OAWCF$_{ex}$ were determined at the reference field size (10 × 10 cm^2) for 6 MV photons with mentioned wedge angles and it was

Table 1: Variations of off-axis correction factor in open fields under reference conditions

(a) For ^{60}Co photon beams

Phantom surface	Field size (cm^2)	Off-axis distance (cm)			
		0	2	3	4
Entrance	10 × 10	1.000	0.998	0.997	0.993
Exit	10 × 10	1.000	0.993	0.990	0.988

(b) For 6 MV photon beams

Phantom surface	Field size (cm^2)	Off-axis distance (cm)			
		0	2	4	6
Entrance	10 × 10	1.000	0.996	0.991	×
Entrance	15 × 15	1.006	1.002	0.997	0.996
Exit	10 × 10	1.000	1.012	1.016	×
Exit	15 × 15	1.005	1.018	1.022	1.026

Table 2: Results of CF$_{f.s,en}$ and CF$_{f.s,ex}$ under reference conditions

(a) For ^{60}Co photon beams

Field size (cm)	5	6	8	10	12	15	18	20
Entrance	1.010	1.045	1.020	1.000	1.000	1.000	0.991	0.989
Exit	1.052	1.046	1.022	1.000	1.000	1.000	0.992	0.988

(b) For 6 MV photon beams

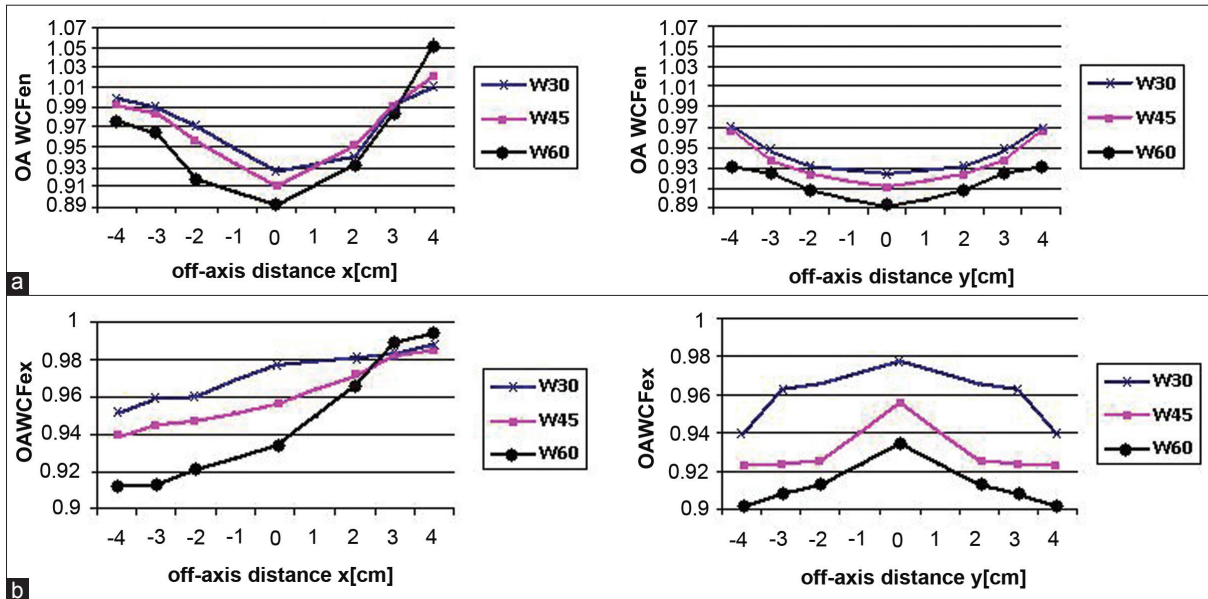| Field size (cm)		5	8	10	12	15	18	20
Entrance		0.986	0.995	1.000	1.003	1.006	1.009	1.010
Exit		0.988	0.995	1.000	1.004	1.005	1.009	1.010

Figure 2: Variations of the OAWCF values at a 10 × 10 cm² field size for ⁶⁰Co photons in the wedged direction (*x*) and in the non-wedged direction (*y*) for three different wedges under reference conditions: (a) for entrance diodes and (b) for exit diodes
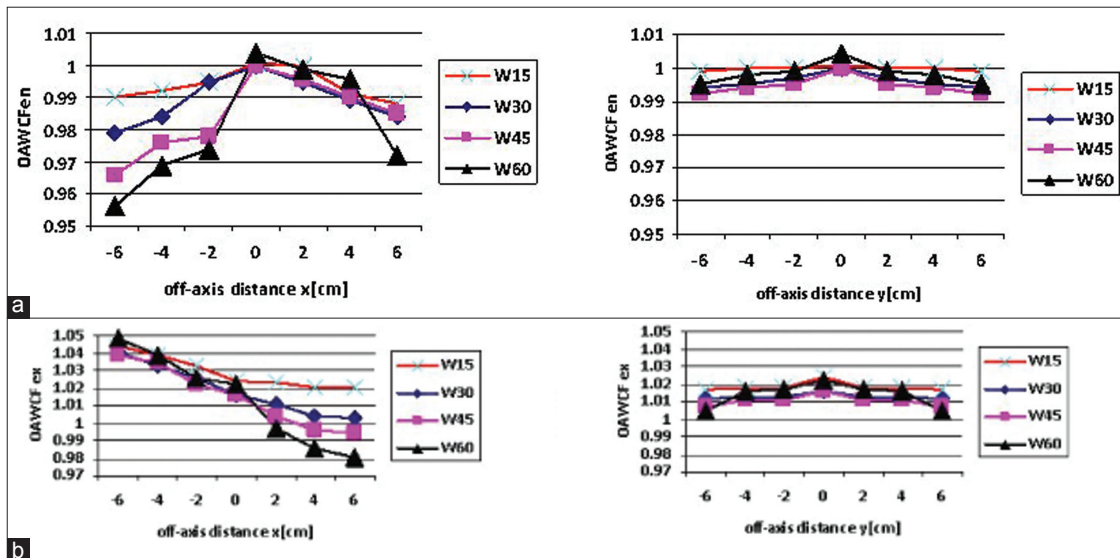

Figure 3: Variations of the OAWCF values at a 15 × 15 cm² field size for 6 MV photons in the wedged direction (*x*) and in the non-wedged direction (*y*) for four different wedges under reference conditions: (a) for entrance diodes and (b) for exit diodes

found that the trend of OAWCF variations at 10×10 cm² field size is similar to that at 15×15 cm² field size (with a slight difference due to corrections of field size).

Field size CF (CF$_{f.s}$)

The entrance and exit field size CFs (CF$_{f.s,en}$ and CF$_{f.s,ex}$, respectively) must be known to account for the difference of diode responses between the reference 10×10 cm² open field size and any other open field sizes. Table 2 shows the CF$_{f.s,en}$ and the CF$_{f.s,ex}$ for various field sizes using the ⁶⁰Co and 6 MV photon beams.

SSD CF (CF$_{SSD}$)

We determined the entrance and exit SSD CFs (CF$_{SSD, en}$

and CF$_{SSD, ex}$, respectively) for ⁶⁰Co and 6 MV photons. Table 3 shows the CF$_{SSD, en}$ and CF$_{SSD, ex}$ for ⁶⁰Co and 6 MV photon beams.

Backscatter CF$_{BS}$

The BSF as a function of the collimator opening was estimated for ⁶⁰Co and 6 MV photon beams on the exit surface of phantom, as shown in [Figure 4].

Thickness CF (CF$_{Z}$)

Figure 5 shows the variations of CF$_{Z}$ for an exit diode exposed to ⁶⁰Co and 6 MV photons when polystyrene phantom thickness increased from 5 to 35 cm.

Table 3: Results of CF$_{SSD,en}$ and CF$_{SSD,ex}$ under reference conditions

(a) For ^{60}Co photon beams

SSD (cm)	65	75	75	80	85	90	95
Entrance	0.973	0.975	0.981	1.000	1.006	1.007	1.012
Exit	1.035	1.029	1.013	1.000	0.994	0.991	0.990

(b) For 6 MV photon beams

SSD (cm)	70	80	90	100	110	120	130
Entrance	0.988	0.991	0.994	1.000	1.004	1.005	1.007
Exit	1.036	1.010	1.004	1.000	0.994	0.992	0.990

Table 4: Comparison of calculated and measured dose values out of central beam axis in the wedged direction [toward the thick edge (+*x*) and toward the thin edge (−*x*) of wedge] and in the non-wedged direction (±*y*) at three positions

Pos. 1	Target dose value (cGy)		
	x = −2 cm	*x* = +2 cm	*y* = ±2 cm
Meas	39.86	31.97	34.98
Cal	39.75	31.82	35.07
Pos. 2	**Target dose value (cGy)**		
	x = −6 cm	*x* = +6 cm	*y* = ±6 cm
Meas	69.90	50.07	58.58
Cal	69.71	50.09	58.31
Pos. 3	**Target dose value (cGy)**		
	x = −4 cm	*x* = +4 cm	*y* = ±4 cm
Meas	26.55	16.22	20.87
Cal	26.52	16.15	20.80

Pos. 1: Photon energy = ^{60}Co, *f.s* = 10 × 10 cm^2, SSD = 70 cm, wedge angle = 45°, *Z* = 10 cm, *d* = 5 cm, off-axis distance = 2 cm, Pos. 2: Photon energy = 6 MV, *f.s* = 18 × 18 cm^2, SSD = 90 cm, wedge angle = 30°, *Z* = 15 cm, *d* = 10 cm, off-axis distance = 6 cm, Pos. 3: Photon energy = 6 MV, *f.s* = 12 × 12 cm^2, SSD = 110 cm, wedge angle = 60°, *Z* = 20 cm, *d* = 15 cm, off-axis distance = 4 cm

Figure 4: The BSF plotted as a function of the field size under reference conditions for ^{60}Co and 6 MV photons (for ^{60}Co energy: SSD = 80 cm, $d_{m,ex}$ = 14.5 cm; for 6 MV energy: SSD = 100 cm, $d_{m,ex}$ = 13.4 cm)

Figure 5: The CF$_z$ plotted as a function of thickness under reference conditions for ^{60}Co (SSD = 80 cm, $d_{m,ex}$ = 14.5 cm) and for 6 MV photons (SSD = 100 cm, $d_{m,ex}$ = 13.4 cm)

Accuracy of algorithm

The results of dose measurements and those calculated from proposed algorithm for three typical positions are presented in [Table 4]. The maximum differences between measured and calculated doses at all point measurements (which are not presented here) were less than 0.5%.

Discussion

According to the results presented in Table 1, maximum deviations of CF$_{off}$ for reference field sizes are within 2%. It means that in off-axis measurements when using open fields, the distance between dosimeter and central beam axis does not have a significant effect on dose determination accuracy by diodes, while considerable deviations in OAWCFs are evident as demonstrated in [Figures 2 and 3]. It can be concluded that in off-axis measurements when using wedged fields, the distance between dosimeter and central beam axis should be considered. This implies on applying a proper OAWCF for wedged fields. This is in agreement with the finding of Huang *et al.* who reported that since it is difficult to put the diode dosimeter at the central axis accurately, a larger
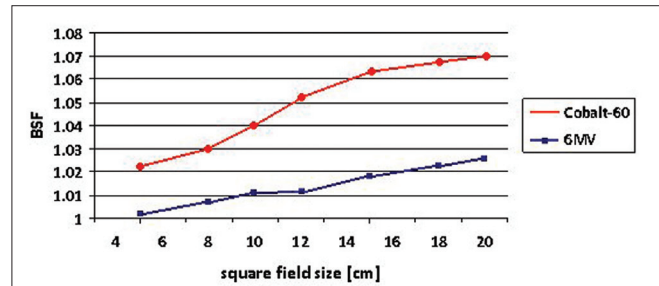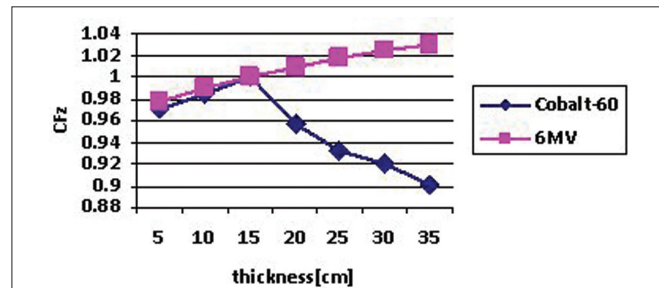
tolerance should be considered for wedged fields when performing *in vivo* dosimetry.[11]

The importance of considering entrance and exit CFs (i.e. field size, SSD, etc.) in the estimation of target dose has been shown in [Tables 2 and 3]. In other words, if one of these factors was not calculated and applied correctly, it would probably cause irreparable faults in tumor dose estimation during *in vivo* dosimetry process.

As shown in Figure 5, variations of thickness CF in ^{60}Co and 6 MV energies have different trends, i.e. maximum variations of thickness correction for ^{60}Co and 6 MV photon beams are 10 and 5%, respectively. It can be attributed to the fact that dose rate decreases for ^{60}Co photons faster than that for 6 MV photons with depth.

The results of dose measurements and calculations using the proposed algorithm, shown in Table 4, illustrate a good agreement between the direct dose measurements using

the ionization chamber and dose calculations using our algorithm, which confirms the validity of the presented algorithm.

Some papers have been published about dose estimation out of central beam axis from surface measurements. In these researches, entrance and exit diodes were positioned on central beam axis and target doses in off-axis positions were obtained by using portal film situated behind the exit surface and applying the related equations.[17,18] The advantage of our proposed algorithm in comparison to the above-mentioned studies is that there is no need to use film dosimeters, thus avoiding the film dosimety problems (i.e. calibration process, film developing, etc.). Also, our algorithm was focused on wedged fields, which differentiated it from other studies.

In some studies, coordinated measurements of entrance and exit doses with diode dosimeters were done to calculate delivered dose to the target using arithmetic mean and geometric methods.[6,16,17,19] In these cases, the arithmetic mean method showed errors within 4%, while the range of errors for the geometric method was within 1.5%. In comparison, the error of our method is within 0.5%. This can be attributed to the fact that in our algorithm, the estimation of delivered dose at exact depth is considered and using approximated depth for target is avoided. On the other hand, dose calculation from entrance and exit diode readings was done in accordance with the real depth of target. While in similar studies,[6,16,17,19] the entrance and exit dose values were averaged via arithmetic methods without consideration of exact depth of target. Thus, the insignificant errors of the dose calculation algorithm in the current study make this *in vivo* dosimetry procedure more effective than the previous investigations.

It is noteworthy that these measurements were carried out only for homogeneous tissue. In our work to be published, the application of the current algorithm to address tissue inhomogeneities in off-axis wedged beams will be demonstrated.

Conclusion

The proposed algorithm in this study is an accurate method for error detection in megavoltage radiotherapy with externally wedged beams. It is concluded that because the OAWCFs' variations for entrance and exit diode dosimeters are totally different in each direction, without applying these factors, systematic errors in the estimation of target dose would be achieved. In summary, it can be concluded from the presented results that diode dosimeters can be used for *in vivo* dosimetry in clinical radiotherapy when using wedged beams.

References

1. Rodriguez MI, Abrego E, Pineda A. Implementation of *in vivo* dosimetry with Isorad semiconductor diodes in radiotherapy treatment of the pelvis. Med Dosim 2008;33:14-21.
2. Tung CJ, Wang HC, Lo HS, Wu JM, Wang CJ. *In vivo* dosimetry for external photon treatments of head and neck cancers by diodes and TLDs. Radiat Prot Dosim 2004;111:45-50.
3. Howlett S, Duggan L, Bazley S, Kron T. Selective *in vivo* dosimetry in radiotherapy using p-type semiconductor diodes: A reliable quality assurance procedure. Med Dosim 1999;24:53-6.
4. Huyskens DP, Bogaerts R, Verstraete J, Loof M, Nystrom H, Fiorino C, *et al*. Practical guidelines for the implementation of *in vivo* dosimetry with diodes in external radiotherapy with photon beams (entrance dose): ESTRO booklet No.5 (Belgium: Garant); 2001.
5. Colussia VC, Beddar AS, Kinsella TJ, Sibata CH. *In vivo* dosimetry using a single diode for megavoltage photon beam radiotherapy: Implementation and response characterization. J Appl Clin Med Phys 2001;2:210-8.
6. Millwater GJ, Macledo AS, Thwaites DI. *In vivo* semiconductor dosimetry as part of routine quality assurance. Br J Radiol 1998;71:661-8.
7. Meijer GJ, Minken AW, Ingen KM, Smulders B, Uiterwall H, Mijnheer B. Accurate *in vivo* dosimetry of a randomized trial of prostate cancer irradiation. Int J Radiat Oncol Biol Phys 2001;49:1409-18.
8. Loncol T, Greffe JL, Vynckeir S, Scalliet P. Entrance and exit dose measurements with semiconductors and thermoluminescent dosimeters: A comparison of methods and *in vivo* results. Radiother Oncol 1996;41:179-87.
9. Leuneus G, Dam JV, Durtex A, Schueren E. Quality assurance in radiotherapy by *in vivo* dosimetry . 2. Determination of the target absorbed dose. Radiother Oncol 1990;19:73-87.
10. Voordeckers M, Goossesns H, Rutten J, Bogeat WV. The implementation of *in vivo* dosimetry in a small radiotherapy department. Radiother Oncol 1998;47:45-8.
11. Huang K, Bice WS, Hidalgo- Salvatierra O. Characterization of an *in vivo* diode dosimetry system for clinical use. J Appl Clin Med Phys 2003;4:132-41.
12. Jornet N, Ribas M, Eudaldo T. *In vivo* dosimetry: Intercomparision between p-type based and n-type based diodes for the 16-25 MV energy range. Med Phys 2000;27:1287-93.
13. Wolff T, Carter S, Langmack KA, Twyman NI, Dendy P. Characterization of a commercial n-type diode system. Br J Radiol 1998;71:1168-77.
14. Saini AS, Zhu TC. Dose rate and SSD dependence of commercially available diode detectors. Med Phys 2004;31:914-24.
15. Mayler U, Szabo JJ. Dose calculation along the nonwedged direction for externally wedged beams: Improvement of dosimetric accuracy with comparatively moderate effort. Med Phys 2002;29:748-54.
16. Nilson B, Ruden BI, Sorcini B. Characterization of silicon diodes as patient dosimeters in external radiation therapy. Radiother Oncol 1998;8:279-88.
17. Huyskens D, Van Dam J, Dutreix A. Midplane dose determination using *in vivo* dose measurements in combination with portal imaging. Phys Med Biol 1994;39:1089-101.
18. Broggi S, Fiorino C, Calandrino R. *In vivo* estimation of mid line dose maps by transit dosimetry in head and neck radiotherapy. Br J Radiol 2002;75:974-81.
19. Van Dam J, Marinello G. Methods for in-vivo dosimetry in external radiotherapy. In: ESTRO booklet series: Physics for clinical

radiotherapy, no.1. Leuven: ESTRO and Garant; 1994.

20. Keall P, Zavgorodni S, Schmidt L, Hascard D. Improving wedged field dose distributions. Phys Med Biol 1997;42:2183-92.

21. Allahverdi M, Geraily G, Esfehani M, Sharafi A, Haddad P, Shirazi A. Dosimetry and verification of ^{60}Co total body irradiation with human phantom and semiconductor diode. J Med Phys 2007;32:169-74.